

多重奈米通道複晶矽薄膜電晶體之製造 與特性研究

研究生:陳稚軒 指導教授:施敏教授 & 張鼎張教授

國立交通大學

電子工程學系 電子研究所碩士班

摘要

本研究主要是在探討具有輕參雜(LDD)與多重通道(multiple channels)結構的複晶矽薄膜電晶體(poly-Si TFTs)，在具有不同通道寬度和數目下，閘極控制能力的好壞，與可靠度的研究。LDD本身具有降低漏電流的效應，結合上十條奈米導線通道的薄膜電晶體，展現出較其他通道數目和寬度的TFT，較佳且較穩定的電性。如較高的開關電流比($>10^8$)，較陡峭的次臨界導通斜率(SS)，較小的汲極導致能障下降(DIBL)，較佳的糾結效應(kink-effect)抑制能力，與較佳的製程穩定度。原因是M10有最佳的閘極控制能力，及較好的電漿保護效應。由一系列的實驗結果發現，閘極的控

制能力是隨著通道數目的增加而變強。此外在可靠度的研究中，M10 的薄膜電晶體展現佳的抗stress的能力，M10 的臨界電壓和次臨界導通斜率幾乎不隨stress時間而改變。因此這種控制能力佳、高效能、高可靠度，且不需額外製程的新穎結構之TFT，將可被廣泛的運用在主動式矩陣液晶顯示器(AMLCD)上



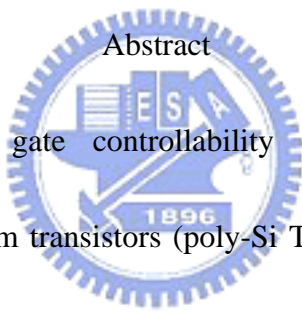
Fabrication and Characterization of Polysilicon Thin Film Transistors with Multiple Nano-wire Channels

Student: Chi-Shen Chen Advisor: Dr. S.M. Sze & Dr. Ting-Chang Chang

Department of *Electronics* &

Institute of Electronics, National Chiao Tung University

Abstract

The logo of National Chiao Tung University is a circular emblem with a gear-like border. Inside the circle, there is a stylized representation of a building or a shield with the letters 'E', 'S', and 'A' arranged vertically. Below this, the year '1896' is inscribed. The logo is positioned behind the abstract text.

We have studied the gate controllability of lightly-doped drain (LDD) polycrystalline silicon thin-film transistors (poly-Si TFTs) with multiple channels and different widths. We deserve that devices with an LDD structure exhibit low leakage current. Additionally, the poly-Si TFT (M10) with ten strips multiple nano-wire channels exhibits the best and the most stable electrical characteristics than all other structures we have studied, such as a higher ON/OFF current ratio ($>10^8$), a steeper subthreshold slope (SS, 110 mV/decade), an absence of drain-induced barrier lowering (DIBL), and a improved suppressed kink-effect. Experiments results show the gate controllability is increasing with channel number from single channel to ten strips multiple channels. The M10 TFT also shows the best stress characteristics, as V_{th} and

SS of the M10 TFT remain constant before and after the stress. Devices with the proposed TFTs are highly promising for use in active-matrix liquid-crystal-display technologies without any additional processes.



致謝

在兩年的碩士生涯中，首先我要由衷的感謝我的兩位指導教授，施敏教授是一個名滿中外的大師級學者，在學術上嚴謹的態度以及對人類文明的貢獻實在是許多青年人甚至是教授們的典範。另外，感謝張鼎張教授給學生一個很寬廣的發揮空間，讓學生能夠充分發揮自己的創意，而張老師對於學術的追求更是一絲不苟；這種對於學術的堅持，更是學生的好榜樣。有機會能接受到兩位老師的指導，實在是學生的福氣，在此獻上最高的敬意與謝意，同時也感謝口試委員的教導與指正，使本論文更完善。另外，也要感謝劉柏村博士、吳永俊、蔡宗鳴、陳紀文、顏碩廷、葉炳宏、陳致宏、陳世青、王敏全..等學長的建議與指導，尤其是吳永俊學長鉅細靡遺的耐心指導更是讓我受益匪淺，對於學長的指導實在是充滿了無限的感激。同時也要感謝在實驗室一起努力的同學和學弟，因為有大家的勉勵和幫助才讓我能順利畢業。此外還要感謝國家奈米元件實驗室提供良好的設備以及研究環境，以及國家奈米實驗室林詩融小姐，在行政上給予充分的幫助。最後我要感謝我的家人的支持，和幫助，讓我能無後顧之憂專心的從事研究，完成我的碩士學位。

Contents

| | |
|--|------|
| Chinese Abstract | I |
| English Abstract | III |
| Acknowledgments (Chinese) | V |
| Contents | VI |
| Table Lists | VII |
| Figure Captions | VIII |
| Chapter 1. Introduction | 1 |
| 1-1. Overview of poly-Si TFT technology | 1 |
| 1-2. Defects in poly-Si film | 3 |
| 1-3. Motivation | 5 |
| Chapter 2. Poly-Si conduction mechanism | 7 |
| 2-1. Transport properties of poly-Si | 7 |
| 2-2. Non-ideal effects | 10 |
| 2-2-1. Leakage current | 11 |
| 2-2-2. Kink effect | 11 |
| 2-2-3. Drain induced barrier lowering (DIBL) | 12 |
| Chapter 3. Experiment | 17 |
| 3-1. Fabrication process of Poly-Si TFT | 17 |
| 3-2. Device parameter extraction | 20 |
| Chapter 4. Experiment results and discussion | 27 |
| 4-1. Gate controllability with different multiple channel number and width of poly-Si TFT | 27 |
| 4-2. Stress effect of MCH and SCH TFTs | 31 |
| Chapter 5. Conclusion | 51 |
| References | 52 |

Table Lists

Chapter 3.

Table I Devices dimension of M10, M5, M2 and S1. All devices have the same active channel thickness 50nm and gate oxide thickness 26nm.

Chapter 4.

Table II Device average and standard deviation parameters of M10, M5, M2 and S1. Number inside the bracket is parameter's standard deviation.

All parameters were extracted at $V_d = 2V$, except for the field-effect mobilities which were extracted at $V_d = 0.05V$.

Table III Variation of experimental electronic parameters and corresponding possible degradation mechanics.

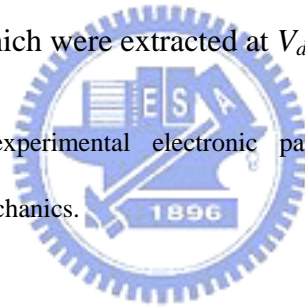


Figure Captions

Chapter 2.

Fig. 2-1 Sketch of the band diagram of the polycrystalline silicon films

Fig. 2-2 A schematic MOSFET cross section, showing the axes of coordinates and the bias voltages at the four terminals for the drain-current model.

Fig. 2-3 Three possible mechanisms of leakage current in poly-Si TFTs, including thermionic emission, thermionic field emission and pure tunneling

Fig. 2-4 The kink effect in the output characteristics of an n -channel SOI MOSFET

Fig. 2-5 Threshold voltage roll-off characteristics in a 0.15 μm complementary metal-oxide-semiconductor (CMOS) field-effect transistor technology.

Fig. 2-6 Calculated surface potential along the channel for n -channel MOSFETs with different channel lengths. The source-channel boundary is at $y = 0$. A low (0.05 V, dotted lines) and a high (1.5 V, solid lines) V_{DS} are applied. Oxide thickness d and substrate doping N_A are 10 nm and 10^{16} cm^{-3} , respectively.

The substrate bias is 0 V

Chapter 3.

Fig. 3-1 The top view of the multiple nano-wire channel

Fig. 3-2 Cross-section view of Fig. 3-1 AA' direction.

Fig. 3-3 One of channel cross-section view of Fig. 3-1

Chapter 4.

Fig. 4-1 (a) Schematic diagram of M10 poly-Si TFT.

(b) Cross-section view of Fig. 1a AA' direction.

(c) One of channel cross-section view of Fig. 1a BB' direction.

Fig. 4-2 (a) Scanning electron microscopy photography of active pattern with the source, the drain and multiple nano-wire channels of M10 TFT. (b) Magnified area of multiple nano-wire channels. The each nano-wire width is 67 nm. (c) Transmission electron microscopy photography of poly-Si grains by solid phase crystallization. The average poly-Si grain size is about 30 nm.

Fig. 4-3 (a) I_d-V_g characteristics of M10 ($L/W = 0.5\mu\text{m}/67\text{nm}\times 10$) poly-Si TFT.

(b) I_d-V_d characteristics of M10 ($L/W = 0.5\mu\text{m}/67\text{nm}\times 10$) poly-Si TFT.

Fig. 4-4 (a) I_d-V_g characteristics of M5 ($L/W = 0.5\mu\text{m}/0.18\mu\text{m}\times 5$) poly-Si TFT.

(b) I_d-V_d characteristics of M5 ($L/W = 0.5\mu\text{m}/0.18\mu\text{m}\times 5$) poly-Si TFT.

Fig. 4-5 (a) I_d-V_g characteristics of M2 ($L/W = 0.5\mu\text{m}/0.5\mu\text{m}\times 2$) poly-Si TFT.

(b) I_d-V_d characteristics of M2 ($L/W = 0.5\mu\text{m}/0.5\mu\text{m}\times 2$) poly-Si TFT.

Fig. 4-6 (a) I_d-V_g characteristics of S1 ($L/W = 0.5\mu\text{m}/1\mu\text{m}$) poly-Si TFT.

(b) I_d - V_d characteristics of S1 (L/W = 0.5um/1um) poly-Si TFT.

Fig. 4-7 Field effect mobility (μ_{FE}) versus different channel number poly-Si TFTs. The dots value present average value and error bars present standard deviation.

Fig. 4-8 Drain current maximum ON/OFF ratio (R) versus different channel number poly-Si TFTs.

Fig. 4-9 Threshold voltage (V_{th}) versus different channel number poly-Si TFTs.

Fig. 4-10 Subthreshold slope (SS) versus different channel number poly-Si TFTs.

Fig. 4-11 Drain current maximum ON/OFF ratio (R) versus different channel number poly-Si TFTs.

Fig. 4-12 Energy-band diagram of top-gate single channel TFT.

Fig. 4-13 Energy band diagram of top-gate M10 TFT. According its tri-gate structure, M10 TFT will include (a) top-gate, and (b) 2 side-gates energy-band diagram.

Fig. 4-14 (a) I_d - V_g characteristics of S1 (L/W = 0.5um/1um) poly-Si TFT, before stress.

(b) I_d - V_g characteristics of S1 (L/W = 0.5um/1um) poly-Si TFT, after stress

time 40 min. with stress condition $V_g = 3V$ and $V_d = 6V$. (c) I_d - V_g

characteristics of S1 (L/W = 0.5um/1um) poly-Si TFT, after stress time 100

min. with stress condition $V_g = 3V$ and $V_d = 6V$. (d) I_d - V_g characteristics of S1

(L/W = 0.5um/1um) poly-Si TFT, after stress time 160 min. with stress

condition $V_g = 3V$ and $V_d = 6V$.

Fig. 4-15 (a) I_d - V_g characteristics of M10 ($L/W = 0.5\mu\text{m}/67\text{nm} * 10$) poly-Si TFT, before stress with stress condition $V_g = 3V$ and $V_d = 6V$. (b) I_d - V_g characteristics of M10 ($L/W = 0.5\mu\text{m}/67\text{nm} * 10$) poly-Si TFT, after stress time 40 min. with stress condition $V_g = 3V$ and $V_d = 6V$. (c) I_d - V_g characteristics of M10 ($L/W = 0.5\mu\text{m}/67\text{nm} * 10$) poly-Si TFT, after stress time 100 min. with stress condition $V_g = 3V$ and $V_d = 6V$. (d) I_d - V_g characteristics of M10 ($L/W = 0.5\mu\text{m}/67\text{nm} * 10$) poly-Si TFT, after stress time 160 min. with stress condition $V_g = 3V$ and $V_d = 6V$.

Fig. 4-16 Field effect mobility (μ_{FE}) of all poly-Si TFTs devices versus different Stress time.

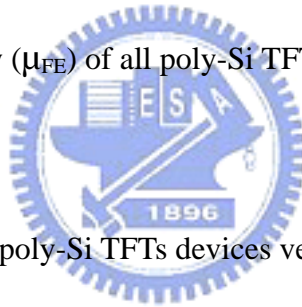


Fig. 4-17 Ion/Ioff ratio of all poly-Si TFTs devices versus different stress time.

Fig. 4-18 Threshold voltage of all poly-Si TFTs devices versus different stress time.

Fig. 4-19 Subthreshold swing (SS) of all poly-Si TFTs devices versus different stress time.